New Journal of Physics
The open access journal at the forefront of physics

Deutsche Physikalische Gesellschaft DPG IOP Institute of Physics

PAPER • OPEN ACCESS

Two-photon induced ultrafast coherence decay of highly excited states in single molecules

To cite this article: Kevin Wilma *et al* 2019 *New J. Phys.* **21** 045001

New Journal of Physics
The open access journal at the forefront of physics

Deutsche Physikalische Gesellschaft DPG
IOP Institute of Physics

Published in partnership with: Deutsche Physikalische Gesellschaft and the Institute of Physics

OPEN ACCESS

RECEIVED
18 December 2018

REVISED
26 February 2019

ACCEPTED FOR PUBLICATION
20 March 2019

PUBLISHED
8 April 2019

PAPER

Two-photon induced ultrafast coherence decay of highly excited states in single molecules

Kevin Wilma[1], Chuan-Cun Shu[2,5], Ullrich Scherf[3] and Richard Hildner[1,4,5]

[1] Soft Matter Spectroscopy, University of Bayreuth, D-95440, Bayreuth, Germany
[2] Institute of Super-Microstructure and Ultrafast Process in Advanced Materials, School of Physics and Electronics, Central South University, Changsha 410083, People's Republic of China
[3] Fachbereich C—Mathematik und Naturwissenschaften and Institut für Polymertechnologie, Universität Wuppertal, D-42097, Wuppertal, Germany
[4] Zernike Institute for Advanced Materials, Nijenborgh 4, University of Groningen, 9747AG Groningen, Netherlands
[5] Authors to whom any correspondence should be addressed.

E-mail: r.m.hildner@rug.nl **and** cc.shu@csu.edu.cn

Keywords: ultrafast spectroscopy, single molecule, conjugated polymers, nanophotonics

Abstract

Coherence is a key aspect of a large variety of processes, ranging from the coherent delocalisation of excitation energy, which is important for energy transfer in supramolecular nanostructures, to coherence between electronic states of a single quantum system, which is essential for quantum optical applications. Coherent control schemes exploit this quantum mechanical property by actively manipulating the outcome of dynamical processes. Moreover, this technique allows measuring dynamical processes under the influence of dephasing. However, going beyond the ensemble averaged situation, i.e. working on the level of single quantum systems, is highly challenging for quantum systems embedded in a solid matrix at elevated temperature. Since interactions between the quantum system and its specific local environment are *a priori* unknown, this requires a reliable approach to retrieve the relevant parameters governing the ultrafast coherent dynamics. Here, we present measurements of the ultrafast coherence decay of two-photon accessible excited states in single organic molecules embedded in a disordered environment at room temperature. We combine this experimental approach with a quantum dynamics identification procedure, which yields a minimum three-level model to describe the obtained data with very good agreement. In particular, we are able to retrieve the ultrafast (coherent) excited state dynamics in single molecules and demonstrate its sensitivity to the local nanoenvironment from molecule to molecule. This work provides a robust approach to measure and analyse ultrafast quantum dynamics in complex nanosystems.

Introduction

To investigate as well as to manipulate ultrafast dynamical processes in nanoscale objects, e.g. single molecules or (in)organic nanostructures, coherent control methods provide capabilities beyond conventional spectroscopic methods [1–9]. Coherent control refers to the active steering of quantum mechanical processes towards a final desired state. This approach involves either the suppression or enhancement of transition probabilities within the system investigated by quantum mechanical interference. Hence, quantum processes that can be addressed with coherent control schemes take place on time scales shorter than the effective dephasing time T_2 [7, 8, 10]. Since in condensed phase at room temperature these time scales are often of the order of some tens of femtoseconds, ultrashort pulsed excitation schemes are required. A further difficulty arises, because in condensed phase the local environment, and thus the dephasing time, is specific for each individual molecule or nanostructure. To understand the intrinsic coherent dynamics on a nanoscale level, ensemble averaging has to be avoided to obtain information about the decoherence properties of each individual system. A combination of coherent control schemes with single-molecule techniques is therefore required [11]. Most coherent control

experiments are based on multi-photon processes [12–14], for which high photostability of the system is a prerequisite owing to relatively high excitation powers. It is thus crucial to develop a reliable technique to induce multi-photon processes in single complex quantum systems, measure them reproducibly, and furthermore analyse the results with high confidence.

Very recently, we have demonstrated that photoluminescence-detected two-photon coherent control schemes can be applied to single organic molecules embedded in a disordered matrix at room temperature [5]. We combined a coherent control experiment on single molecules, exploiting phase-shaped single-pulse excitation schemes, with a quantum dynamics identification (QDI) procedure. This approach allowed us to retrieve the excited state energy landscape for each molecule. Moreover, we were able to resolve transitions into a 'hidden' highly excited state that is not connected to a photoluminescent channel.

Here, we focus on the ultrafast coherence dynamics of a two-photon accessible excited state in single molecules at room temperature. We employ amplitude-shaped double-pulse sequences to measure the two-photon induced coherence decay of highly excited states of the conjugated polymer methyl-substituted ladder-type poly(*para*-phenylene), MeLPPP. Analysing these data with the QDI procedure, we find that in single molecules the high-lying excited state features a rapid coherence decay with an average dephasing time of 75 fs. In addition, we demonstrate that from this two-photon allowed state rapid population relaxation within about 150 fs occurs into the photoluminescent lowest excited singlet state. The distributions of both times are widely spread due to varying local interactions between each molecule and its specific disordered matrix.

Materials and methods

The detailed concept of our experimental and theoretical approach was already introduced in [5]. Single-molecule samples were prepared by dissolving MeLPPP (molecular weight $M_n = 55300$ Da) in toluene (Sigma-Aldrich, 99.7%) at a concentration of 10^{-9} M containing 5 mg ml^{-1} polystyrene. Spincoating of this solution onto a freshly cleaned quartz cover slip yields samples with thickness of several 100 nm and spatially well-isolated individual MeLPPP-molecules. In our single-molecule experiment we exploit that, owing to the ladder-type backbone, MeLPPP possesses a very rigid structure. Thus a high degree of symmetry is preserved even in a solid matrix. Hence, the electronic states of MeLPPP possess alternating even and odd parity, resulting in mutually exclusive one-photon and two-photon allowed transitions from the electronic ground state S_0 into excited electronic states [15, 16]: One-photon allowed (but two-photon forbidden) optical transitions occur into the lowest excited state S_1, and two-photon (but one-photon forbidden) transitions can be induced with high efficiency into the higher lying excited state S_2, respectively (see figure 1(a)). After two-photon excitation into S_2 rapid population relaxation into S_1 takes place within typically 150 fs, from where photoluminescence can be detected, i.e. the photoluminescence from single MelPPP molecules is directly proportional to the two-photon transition probability from S_0 into S_2.

We use a Ti:Sapphire oscillator (Griffin-10-WT, KMLabs) to generate ultrashort pulses with a Fourier-transform limited width of about 40 fs (400 cm^{-1} or 20 nm spectral bandwidth). Its output spectrum is centred at a photon energy $\omega_0 = 13000$ cm^{-1} (770 nm), which allows to induce non-resonant two-photon transitions into the second excited state S_2 of MeLPPP located at about 26400 cm^{-1}. A pulse shaper (MIIPS-HD, Biophotonic Solutions) is used to compensate dispersions induced by the optical elements [17, 18], see appendix A for the pulse characterisation. A pair of identical time-delayed, phase-locked pulses is created via simultaneous amplitude and phase shaping by a liquid crystal display spatial light modulator using home-written modulation masks. The applied modulation reads $A(\omega) = |\cos\{0.5[(\omega - \omega_0)\tau + \Delta\phi]\}|$ for the amplitude and $\Phi(\omega) = 0.5\pi\ \mathrm{sgn}(\cos\{0.5[(\omega - \omega_0)\tau + \Delta\phi]\})$ for the phase mask, where sgn is the sign function, $\Delta\phi = 0$ and the time delay τ was varied between 0 and 300 fs in 6 fs steps. For each measurement the time-averaged excitation power at the sample plane was constant at 2.5 mW for all delays. These pulse pairs are directed to the sample and focussed onto single MeLPPP molecules by an objective with low numerical aperture (NA = 0.5). The photoluminescence signal is collected in transmission by a second objective (NA = 0.85) and separated from the excitation light by two BG 39 colour glass filters (Schott) and one shortpass filter (filter edge at 492 nm, AHF). Finally, the delay-dependent photoluminescence is detected with a single-photon sensitive photodiode (PDM, Micro Photon devices). The coherence decay was measured by varying the delay from 0 fs to 300 fs, while keeping the inter-pulse phase difference constant at $\Delta\phi = 0$ rad. All experiments were carried out at room temperature under ambient conditions.

The obtained delay-dependent photoluminescence signals are analysed by our QDI procedure, which yields information about the energy landscape of each molecule and the ultrafast relaxation and dephasing dynamics of the quantum states involved. In this present work, the simulations yield a minimum three-level model, that consists of S_0, S_1 and S_2 with corresponding energies E_0, E_1 and E_2. To describe the underlying quantum processes we model single molecules as open quantum systems, including the dissipative influence of a non-

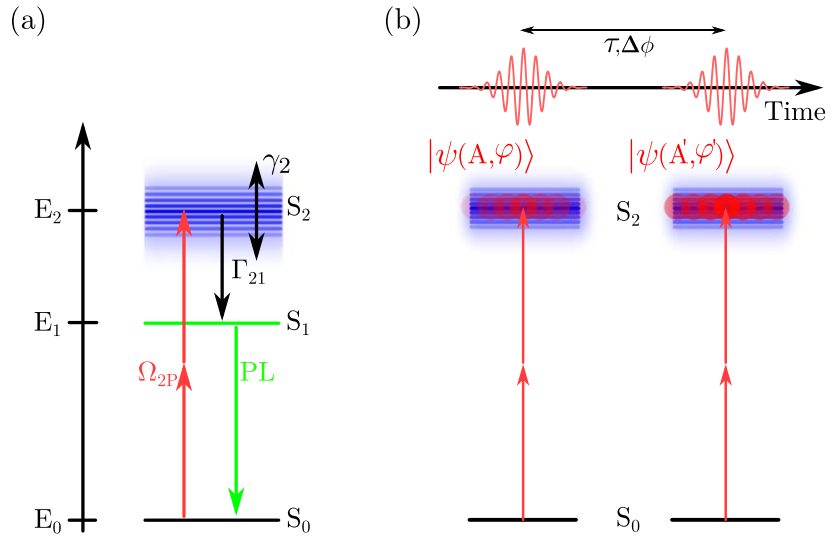

Figure 1. Measurement of the coherence decay of single molecules. (a) Energy level diagram of the involved states of the conjugated polymer MeLPPP, with Ω_{2P} describing the two-photon Rabi coupling between the molecule and the excitation field, γ_2 the dephasing of the two-photon accessible second excited state S_2, Γ_{21} the relaxation into the (two-photon forbidden, but one-photon allowed) first excited state S_1, and PL the photoluminescence. (b) A double pulse sequence with variable delay τ and constant phase difference $\Delta\phi$ generates population (red full circles) in the second excited electronic state S_2 by a two-photon transition. The population of S_2, and thus of the photoluminescent state S_1, is dependent on the delay τ between the pulses as well as the dephasing and relaxation of state S_2, (indicated by the full circles).

Markovian local environment. In this situation the time-dependent evolution of the density matrix of the three states is calculated by the Lindblad master equation [19]

$$\dot{\rho}(t) = \frac{-\mathrm{i}}{\hbar}\left[\begin{pmatrix} E_0 & 0 & -D_{21}^2 R[E^2(t)] \\ 0 & E_1 & 0 \\ -D_{12}^2 R(E^2(t)) & 0 & E_2 \end{pmatrix}, \rho(t)\right] + L_{21}(\rho(t)) + D_2(\rho(t)),$$

where $D_{12} = D_{21}$ denotes the two-photon transition dipole moment. The first summand on the right-hand side in this master equation reflects the interaction of the external time-dependent electric field with the two-photon dipole moment of the quantum system. The time-dependent electric laser field $E(t)$ can be obtained by

$$E(t) = \frac{1}{\sqrt{2\pi}} \int_0^{\text{infinity}} A(\omega) \left| \cos\left(\frac{1}{2}(\omega - \omega_0)\tau\right) \right| \mathrm{e}^{\mathrm{i}\frac{\pi}{2}\mathrm{sign}\left(\cos\left(\frac{1}{2}(\omega-\omega_0)\tau\right)\right)} \mathrm{e}^{-\mathrm{i}\omega t} \mathrm{d}\omega,$$

with the experimentally measured amplitude $A(\omega)$ of the laser spectrum, which leads to the two-photon Rabi frequency $\Omega_{2P} = D_{12}^2\varepsilon_0^2$ with the peak strength of the electric field ε_0. The Lindblad operator $L_{21} = \Gamma_{21}(\rho_{22}|1><1|-1/2\{|2><2, \rho\})$ describes the population relaxation from S_2 to S_1 with a rate of Γ_{21}, which is typically of the order of 100 fs for highly excited states in organic molecules [20]. The superoperator $D_2 = \gamma_2(\rho_{22}|2><2|-1/2\{|2><2|, \rho\})$ describes dephasing of state S_2 with a rate of γ_2, which is usually some tens of femtoseconds at room temperature due to interaction with the disordered local environment [11]. The brackets $|1>$ and $|2>$ represent the eigenvectors of S_1 and S_2, respectively. Since the local surrounding of single molecules varies from molecule to molecule, the corresponding variations in interactions with the environment will lead to a distribution of the parameters Ω_{2P}, E_1, E_2, Γ_{21} and γ_2. To this end, a multi-parameter optimisation problem is solved to identify a set of these free parameters within the minimal three-level model. More details of the QDI procedure can be found in [5]. To calculate the coherence decays, a snapshot of the populations and coherences is taken 400 fs after the second pulse in each sequence. In analogy to our recent work [5], in figures 2(a)–(c) the solid lines represent the sum of the populations in states S_2 and S_1 owing to the fast population relaxation from S_2 to S_1.

Results and discussion

The idea for the detection of quantum coherence between the electronic ground state S_0 and the two-photon accessible, second excited state S_2 of single MeLPPP molecules is shown in figure 1(b). We exploit constructive quantum interference between the excitation pathways generated by the sequence of phase-locked pulse pairs ($\Delta\phi = 0$) [7]. The interaction with the first excitation pulse induces population transfer from S_0 to S_2 via a two-photon process and creates quantum coherence, i.e. a superposition of wave functions of the states S_0 and S_2.

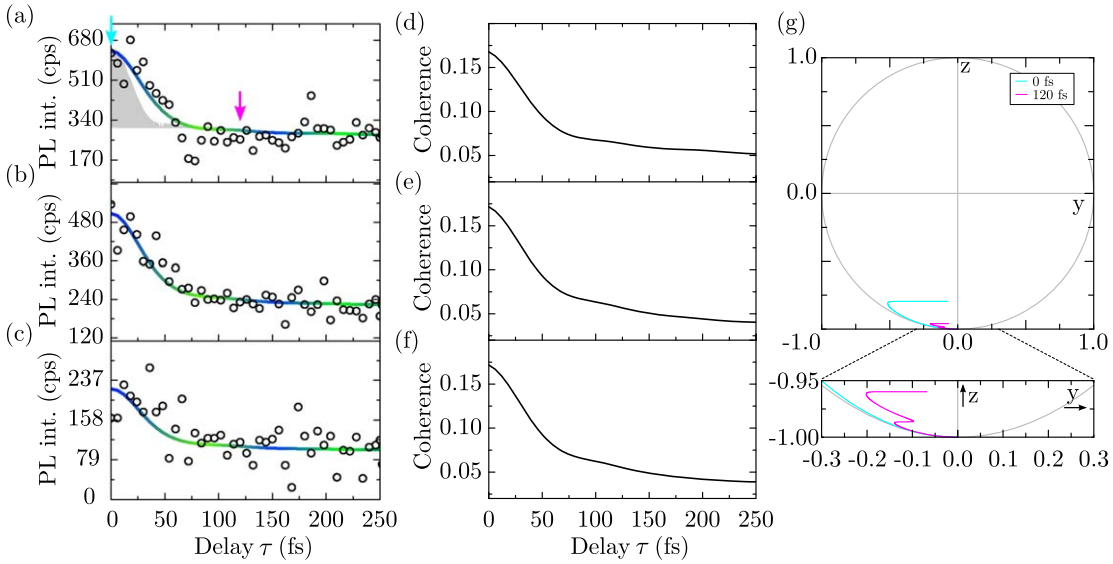

Figure 2. Coherence decay and quantum optical operations with single molecules. (a)–(c) Coherence decay data sets of three different individual MeLPPP molecules 1, 2, and 3, respectively (black circles) as function of the inter-pulse delay at constant inter-pulse phase difference. The grey filled area in (a) reflects the collinear intensity autocorrelation envelope of the excitation pulse. The results of the quantum dynamics identification procedures are overlaid as blue–green lines, and correspond to the sum of populations in state S_1 and S_2 (see methods). Values of optimal parameters for molecules 1, 2, and 3: $E_2 = 26010\ \mathrm{cm}^{-1}, 25951\ \mathrm{cm}^{-1}, 25947\ \mathrm{cm}^{-1}$, $\gamma_2 = 1/77\ \mathrm{fs}^{-1}, 1/72\ \mathrm{fs}^{-1}, 1/52\ \mathrm{fs}^{-1}$ and $\Gamma_{21} = 1/146\ \mathrm{fs}^{-1}, 1/155\ \mathrm{fs}^{-1}, 1/264\ \mathrm{fs}^{-1}$. (d)–(f) Delay dependent coherence $y = i \cdot (\rho_{20} - \rho_{02})$ between the electronic ground state S_0 and the second excited state S_2 for the corresponding data shown in (a)–(c). (g) Time-dependent projection of the Bloch vector tip onto the y–z-plane for two different delays (turquoise 0 fs, magenta 120 fs) for molecule 1 (figure 2(a)). Bottom: expanded region of the Bloch sphere from y: −0.3 to 0.3 and z: −1.0 to −0.95.

The phase of the wave function describing this superposition state is determined by that of the first excitation pulse. In the time interval between the pulses, this coherence will decay (the phase memory will be lost) due to electronic dephasing processes caused by interactions with the local surrounding. If for a given delay τ coherence still persists, the second, phase-locked pulse increases the excited state population of S_2 by constructive quantum mechanical excitation pathway interference. If the delay exceeds the coherence time $1/\gamma_2$, however, phase coherence in the system is completely lost, excitation pathway interference does not take place any more, and the excited state population converges to the incoherent level. This decay of coherence and thus of population transfer into state S_2 as function of the delay is then reflected in a decay of the detected PL signal of each molecule. Analysis of this delay-dependent decay of the PL signal allows to determine ultrafast electronic dephasing and population relaxation dynamics in highly excited states of single molecules at room temperature.

Examples of measured coherence decays are shown in figures 2 (a)–(c) for three different single MeLPPP molecules 1, 2, and 3, respectively. The detected PL-signal decays with increasing delay to a constant value after $\tau = 50$–100 fs. This observation indicates a rapid loss of coherence between S_0 and S_2 due to the dephasing influence of the environment combined with fast population relaxation from S_2 to the photoluminescent state S_1 [21, 22] (see also below). To demonstrate that the recorded delay-dependent PL traces can indeed be attributed to the coherence decay, i.e. to molecular dynamics, we further plot the envelope of the collinear intensity autocorrelation of our pulse (grey filled area in figure 2(a)), which is clearly shorter than the measured PL decay (see the collinear autocorrelation function in appendix A, figure A1). A further control experiment is described in appendix B (figure B1), where we depict the phase-dependent variation of the two-photon induced PL of MeLPPP at a constant delay time of 70 fs, i.e. after complete decay of the pulse autocorrelation function.

We now use the QDI procedure with the minimal three-level model to reproduce these measured delay-dependent traces in figures 2(a)–(c). To perform the simulations, the energy of the electronic ground state S_0 was set to $E_0 = 0\ \mathrm{cm}^{-1}$ and that of state S_1 was kept constant at $E_1 = 22000\ \mathrm{cm}^{-1}$, which is justified because S_1 is not optically addressed by the laser pulses. Initial values in the QDI procedure for the free parameters were $\gamma_2 = 1/75\ \mathrm{fs}^{-1}$ for the dephasing rate, $\Gamma_{21} = 1/150\ \mathrm{fs}^{-1}$ for the population relaxation, and $E_2 = 26000\ \mathrm{cm}^{-1}$ for the energy of S_2. Moreover, the QDI was carried out for a Rabi-coupling fixed at $\Omega_{2P} = 120\ \mathrm{cm}^{-1}$ for the $S_0 \rightarrow S_2$ transition, because we found that the simulations are not sensitive to the precise value of Ω_{2P}. Minimising the residuals between data and simulations the QDI procedure identifies the optimised parameters for this minimal model. We find very good agreement between the measured PL and the output of the QDI procedure for the optimised values that are given in the caption of figures 2(a)–(c) for each molecule. For molecules 1 and 2 dephasing rates are around $1/75\ \mathrm{fs}^{-1}$, relaxation rates of approximately $1/150\ \mathrm{fs}^{-1}$ were retrieved, and we find near-resonance of E_2 with the doubled excitation energy of 26 000 cm^{-1}. Molecule 3, in

contrast, exhibits dynamics considerably different with a faster dephasing rate of $1/52$ fs^{-1} and a slower relaxation rate of $1/264$ fs^{-1}. These examples show that all free parameters strongly vary between different measurements, and that the disordered local surrounding of each molecule has a strong impact on the ultrafast response.

Since within the QDI procedure the molecular dynamics is described by the Lindblad master equation, we have direct access to all time dependent density matrix elements ρ_{00} and ρ_{22} (populations), as well as ρ_{02} and ρ_{20} (coherences) for states S_0 and S_2. The coherence term, defined here as $y = i \cdot (\rho_{20} - \rho_{02})$, is shown as function of the delay τ in figures 2(d)–(f). For all molecules the decay of the coherence resembles the decay of the excited state population with a rate of γ_2 (see figure caption). This behaviour further corroborates that the loss of coherence between the S_0 and S_2 wave functions is the predominant process causing the PL decay shown in figures 2(a)–(c). Population relaxation from S_2 to S_1 takes place on slower timescales and thus has a much smaller effect on the overall shape of the PL signals.

The time-dependent information about the density matrix elements allows us to visualise the molecular dynamics by the motion of the Bloch vector on the Bloch sphere during interaction of the molecule with a pair of time-delayed, phase-locked pulses. Using the coherence y introduced above and the population term, defined as $z = (\rho_{22} - \rho_{00})$, the position of the tip of the Bloch vector projected onto the y–z plane can be calculated. The z-component describes the population of state S_2 and dynamics parallel to the y-axis (at constant z) are due to dephasing effects. For molecule 1 this Bloch vector trace is plotted in figure 2(g) for two different delays $\tau = 0$ fs and 120 fs (marked with the coloured arrows in figure 2(a)). At a delay of $\tau = 0$ fs the trace of the Bloch vector tip shows that a maximum of 20% of population is transferred from the ground state to S_2 (turquoise curve). At $\tau = 120$ fs dephasing in the time interval between the pulses already affects the overall population transfer from S_0 to S_2, see the intermediate 'horizontal' motion of the Bloch vector tip in the magenta curve, inset figure 2(g). Hence, the population transferred from state S_0 to state S_2 decreases with increasing delay due to the loss of coherence in the time interval between the pulses.

We note, however, that the Bloch plot cannot reproduce all details, e.g. the measured contrast of 2 between the PL signal (and thus S_2 population) at 0 fs delay (turquoise) and e.g. at 120 fs (magenta). This discrepancy is due to the fact, that the populations shown in (a)–(c) are the sum of populations of states S_1 and S_2, because all population created in S_2 will relax into photoluminescent state S_1 within the excited state lifetime of S_1 ($>$ 100 ps). In contrast, the Bloch plot reflects the dynamics only of state S_2, and efficient and fast $S_2 \rightarrow S_1$ relaxation with time constants of $\sim$150 fs is not reflected. Nevertheless, this Bloch representation clearly demonstrates that two-photon induced quantum optical operations on femtosecond time scales on a single molecule are feasible.

The QDI analysis was carried out on the measured coherence decays of 30 MeLPPP molecules and the obtained results are summarised in the histograms in figure 3. The maximum of the energy E_2 of the two-photon accessible state S_2 is spread around 26 000 cm^{-1} with a width of 400 cm^{-1}. Note that the width of this histogram does clearly not reflect that of the actual distribution of energies of S_2, but rather the laser bandwidth. The actual distribution of E_2 can be expected to be much broader with a FWHM of around 800 cm^{-1} as estimated from ensemble two-photon spectra [15]. The narrow distribution about the doubled laser energy is reasonable, however, because in single-molecule experiments usually only those emitters will be detected with the highest PL signal, which requires most efficient excitation conditions, i.e. we detect only the 'most resonant' molecules. Furthermore, we find that the dephasing time is spread between 50 and 120 fs with a maximum around 75 fs. These dephasing times are in agreement with those obtained by pure phase-dependent measurements of the same conjugated polymer as we have reported recently. Moreover, these are in line with the line widths of single MeLPPP molecules at room temperature [21], although this line width was determined from the PL spectra from state S_1 and not for state S_2. Finally, the distribution of time constants for the relaxation from S_2 to the photoluminescent state S_1 ranges from 100 to 260 fs, which is distributed around the value of 150 fs determined by ensemble pump-probe experiments [22]. This population relaxation—a process referred to as internal conversion—depends on the overlap of vibrational wave functions of the vibrationless state S_2, which we directly excite by the two-photon process, with an accepting, isoenergetic vibrational mode in S_1, and on the energy difference between S_2 and S_1 (the so-called energy gap law) [20]. The observed large variations in relaxation times are therefore in line with the distribution of the energy of state S_2.

Conclusion

We demonstrated the first ultrafast, two-photon induced measurements of the coherence decay of individual organic molecules that are embedded in a complex, disordered environment at room temperature. We note that based on the ergodic principle the coherence decay detected here for single molecules can be identified with the envelope of the optical free-induction decay, as discussed in detail in [7]. Our data were analysed using a QDI procedure, which revealed a strong variation of photophysical parameters from molecule to molecule. In

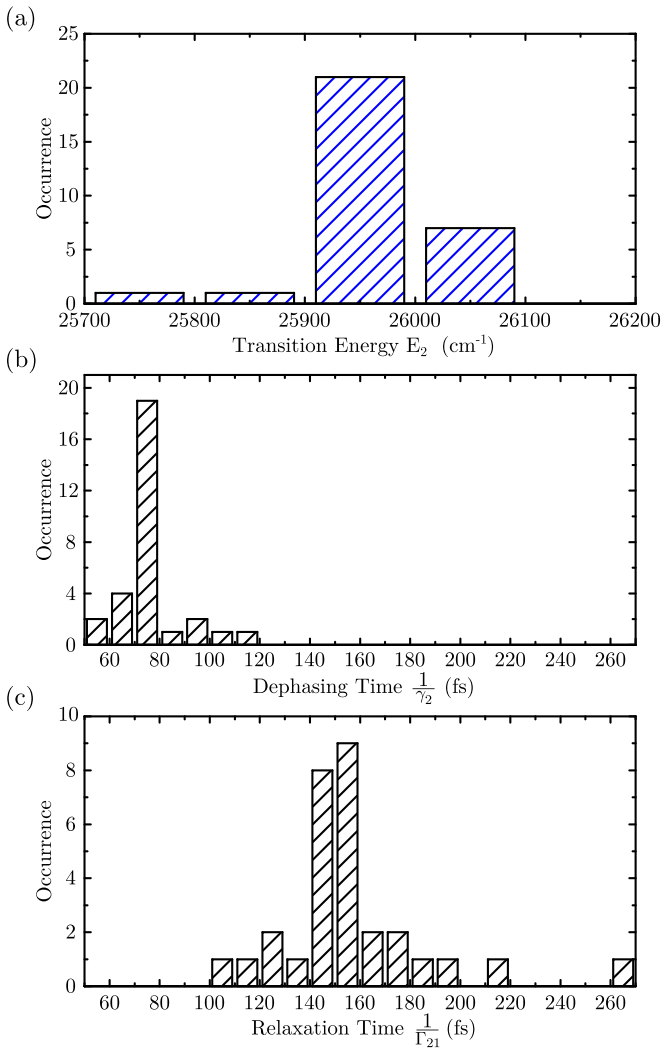

Figure 3. Statistics obtained by the QDI procedure for 30 MeLPPP molecules. (a) Transition energy E_2 distribution from the electronic ground state S_0 to the two-photon accessible electronic state S_2. (b) Statistics of the dephasing time $1/\gamma_2$. (c) Statistics of the relaxation times $1/\Gamma_{21}$ between the second excited S_2 and the first excited state S_1.

particular, we revealed the dephasing time of a higher excited state as well as the relaxation time into the lower lying photoluminescent state. The broad distribution of dephasing and relaxation times found here is largely determined by the strongly varying interactions between each molecule investigated with its local, disordered environment. These changes in interactions strongly impact on the energy landscape as well as on the ultrafast intra-molecular dynamics. Our combined experimental-theoretical approach represents a powerful, reliable tool to study ultrafast dynamics of nanostructured systems in complex surroundings under ambient conditions.

Acknowledgments

KW and RH acknowledge financial support from the German Research Foundation (DFG) through projects HI1508/3 and GRK1640. RH was also supported by the Elitenetzwerk Bayern (ENB, elite study programme *Macromolecular Science*). CCS acknowledges financial support from the National Natural Science Foundation of China (NSFC) under Grant No. 61803389.

Appendix A

In figure A1 we present the experimental characterisation of the excitation pulse: (a) depicts the amplitude of the laser spectrum, in (b) the Multiphoton Intrapulse Interference Phase Scan (MIIPS) [17, 18] of the compressed pulse at the sample plane is displayed; (c) shows the collinear intensity autocorrelation, detected by second harmonic generation, revealing a pulse width of about 30 fs (full width at half maximum).

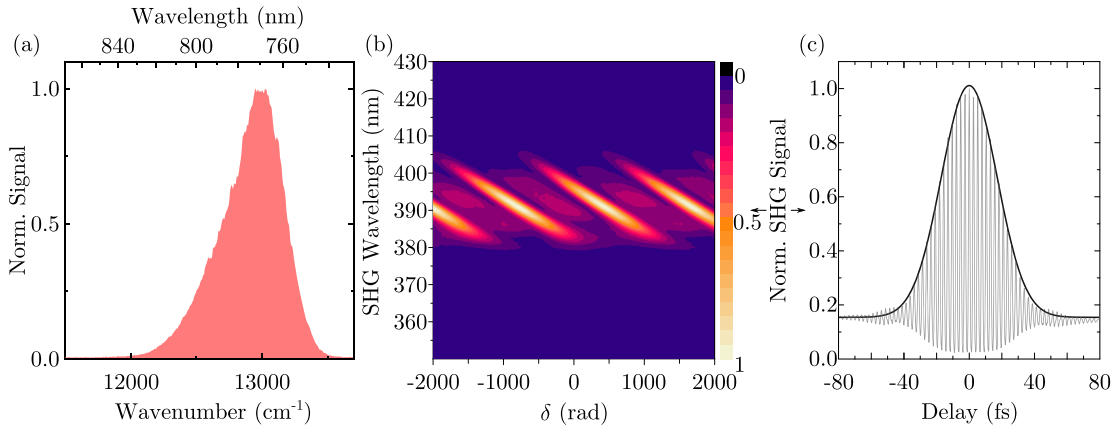

Figure A1. Characterisation of the excitation pulses. (a) Spectral intensity of the output of the Ti:Sa-laser centred at 13000 cm^{-1} and a full width at half maximum of 400 cm^{-1}. (b) Normalised multiphoton intrapulse interference phase scan (MIIPS) of the compressed pulse at the sample plane, detected by second harmonic generation (SHG) in a BBO-crystal. (c) SHG detected collinear intensity autocorrelation of the compressed excitation pulse. The width of 41 fs of the autocorrelation translates into a pulse width of ca. 30 fs assuming a Gaussian pulse shape.

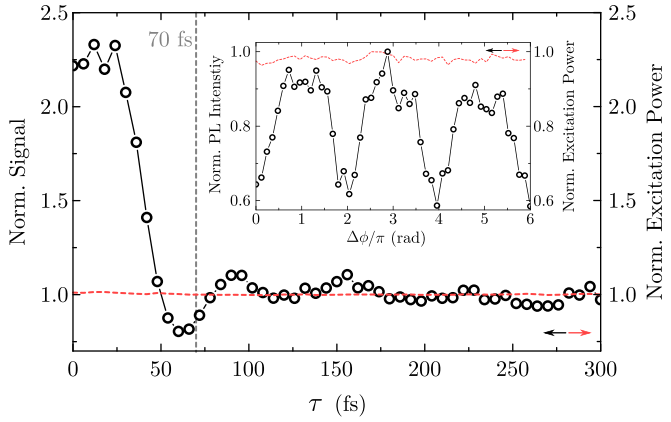

Figure B1. Coherence decay and phase scan on a MeLPPP ensemble. Coherence decay of an ensemble of MeLPPP dissolved in toluene at room temperature (open circles, $\Delta\phi = 0$ rad) and normalised time-averaged excitation power (red dashed). The grey dashed line marks $\tau = 70$ fs. Inset: Scan of the phase-parameter $\Delta\phi$ for a fixed delay of 70 fs (open circles) and normalised excitation power (red dashed).

Appendix B

In order to proof the existence of coherence inherent to MeLPPP we show in figure B1 the ensemble coherence decay of MeLPPP dissolved in toluene at room temperature. The PL intensity rapidly decays within the first 50 fs and exhibits a strong periodic modulation on top of the trace for delays up to 200 fs ($\Delta\phi = 0$ rad). This periodic modulation is due to the detuning between the doubled centre frequency of the excitation pulses (2·13000 cm^{-1}) and the ensemble absorption of the two-photon allowed state S_2 (26 380 cm^{-1} [15]). The existence of this beating at delays longer 50 fs is already a strong indication for the long living coherence.

This is further corroborated by the measurement shown in the inset, for which we varied the inter-pulse phase difference $\Delta\phi$ in steps of 0.12 π at a fixed delay time of $\tau = 70$ fs. These data feature a clear contrast of almost 40% between the maximum and the minimum signal (note that the non-sinusoidal variation stems from the detuning). At a delay of 70 fs possible artefacts due to intensity autocorrelation of the excitation can be excluded (figure A1(c)) and all observed effects can be ascribed to intra-molecular properties.

The red dashed lines in figure B1 represent the normalised time-averaged excitation power for each measurement that was monitored simultaneously.

ORCID iDs

Richard Hildner https://orcid.org/0000-0002-7282-3730

References

[1] Brumer P and Shapiro M 1986 *Chem. Phys. Lett.* **126** 541–6
[2] Shapiro M and Brumer P 2003 *Rep. Prog. Phys.* **66** 859–942
[3] Aeschlimann M *et al* 2007 *Nature* **446** 301–4
[4] Higgins G, Pokorny F, Zhang C, Bodart Q and Hennrich M 2017 *Phys. Rev. Lett.* **119** 220501
[5] Wilma K, Shu C, Scherf U and Hildner R 2018 *J. Am. Chem. Soc.* **140** 15329–35
[6] Hildner R, Brinks D, Nieder J B, Cogdell R J and van Hulst N F 2013 *Science* **340** 1448–51
[7] Hildner R, Brinks D and Hulst N F V 2011 *Nat. Phys.* **7** 172–7
[8] Weigel A, Sebesta A and Kukura P 2015 *J. Phys. Chem. Lett.* **6** 4032–7
[9] Mittal R, Glenn R, Saytashev I, Lozovoy V V and Dantus M 2015 *J. Phys. Chem. Lett.* **6** 1638–44
[10] Accanto N *et al* 2017 *Light Sci. Appl.* **6** e16239
[11] Zewail A H 1980 *Acc. Chem. Res.* **13** 360–8
[12] Meshulach D and Silberberg Y 1999 *Phys. Rev.* A **60** 1287–92
[13] Meshulach D and Silberberg Y 1998 *Nature* **396** 239–42
[14] Liebel M and Kukura P 2016 *Nat. Chem.* **9** 45–9
[15] Hildner R, Lemmer U, Scherf U and Köhler J 2007 *Chem. Phys. Lett.* **448** 213–7
[16] Hohenau A, Cagran C, Kranzelbinder G, Scherf U and Leising G 2001 *Adv. Mater.* **13** 1303–7
[17] Lozovoy V V, Pastirk I and Dantus M 2004 *Opt. Lett.* **29** 775
[18] Xu B, Gunn J M, Dela Cruz J M, Lozovoy V V and Dantus M 2006 *J. Opt. Soc. Am.* B **23** 750
[19] Lindblad G 1976 *Commun. Math. Phys.* **48** 119
[20] Köhler A and Bässler H 2015 *Electronic Processes in Organic Semiconductors: An Introduction* (Weinheim: Wiley)
[21] Hildner R, Lemmer U, Scherf U and Köhler J 2006 *Chem. Phys. Lett.* **429** 103–8
[22] Harrison M G *et al* 1999 *Chem. Phys. Lett.* **313** 755–62